

Vortex replication in Bose-Einstein condensates trapped in double-well potentials

José R. Salgueiro,¹ M. Zacarés,² H. Michinel,¹ and A. Ferrando³

¹Área de Óptica, Facultade de Ciencias de Ourense, Universidade de Vigo, As Lagoas s/n, 32004 Ourense, Spain

²Instituto Universitario de Matemática Pura y Aplicada, Universidad Politécnica de Valencia,

Camino de Vera s/n, 46022 Valencia, Spain

³Departamento de Óptica, Interdisciplinary Modeling Group InterTech, Universidad de Valencia, Dr. Moliner 50, 46100 Burjassot (Valencia), Spain

(Received 20 July 2008; revised manuscript received 17 November 2008; published 30 March 2009)

In this work we demonstrate, by means of numerical simulations, the possibility of replicating matter-wave vortices in a Bose-Einstein condensate trapped in a double-well potential. The most remarkable result is the generation of replicas of an initial vortex state located in one side of the double potential, which evolves into two copies, each one located in one of the potential minima. A simple linear theory gives the basic explanation of the phenomenon and predicts experimental realistic conditions for observation. A complementary strategy of easy experimental implementation to dramatically decrease the replication time is presented and numerically tested for the general case of nonlinear atomic interactions.

DOI: [10.1103/PhysRevA.79.033625](https://doi.org/10.1103/PhysRevA.79.033625)

PACS number(s): 03.75.Lm, 05.45.-a, 74.50.+r

I. INTRODUCTION

The behavior of topological defects in a medium with a broken symmetry is of fundamental interest in superconductivity, superfluidity, and nonlinear optics. In a wave field, vortices can be generated by several means, which include rotation of an anisotropic potential [1,2] or phase imprinting methods [3] in the case of trapped ultracold atomic gases.

Most of the literature in relation with vortices in Bose-Einstein condensates (BEC) in gases is devoted to static properties such as lattices [4,5] or fluctuations around a fixed position [6,7]. Less attention has been paid to moving vortices as it is intrinsically difficult to control the vortex path in usual experiments. The problem of vortex motion on gradually varying backgrounds can be studied analytically using the method of matched asymptotic expansions [8]. Unfortunately, there is no universal mobility relation so the detailed asymptotic expansion procedure has to be carried out for each particular system [9].

In the present work we will study vortex motion through a double-well structure, which is an important and well-known technique in BEC setups that has been used to study, among other experiments, Josephson junctions [10–12] and matter-wave interference phenomena [13–15]. We will demonstrate by means of numerical simulations the possibility of tunneling matter-wave vortices in a Bose-Einstein condensate trapped in a double-well potential. The most remarkable effect found is the possibility of generating replicas of an initial vortex state (located in one side of the double potential), which can be made to evolve into two copies, each one located in one of the potential minima. A simple linear theory gives the basic explanation of the phenomenon and predicts experimental realistic conditions for observation. Our results generalized the particular problem of replicating a fundamental BEC state to the case of vortices, opening the door to experiments which are easy to implement with the current technology.

We will consider a planar condensate, i.e., strongly confined in the Z direction by an harmonic potential V_z

$=m\omega_z^2 Z^2/2$, m being the atom mass and ω_z the trapping frequency, so that it can be considered effectively two dimensional. In this situation we can describe the dynamics of the condensate as given by a wave function $\Psi(\mathbf{r}, t)$, dependent on the spatial variables $\mathbf{r}=(X, Y, Z)$ and time t , which can be factorized in the form [16] $\Psi(\mathbf{r}, t)=\Phi_0(Z)\Phi(X, Y, t)$. We define a time variable $\tau=\omega_z t$, so that it is now measured in units of the inverse of the trapping frequency ω_z , and also normalized spatial variables after rescaling by the cloud size along z , $(x, y, z)=(X, Y, Z)/r_z$, being $r_z=\sqrt{\hbar/(2m\omega_z)}$. We also define a dimensionless wave function $\psi(x, y, \tau)=r_z\Phi(X, Y, t)$, which should satisfy

$$i\frac{\partial\psi}{\partial\tau}=-\nabla_{\perp}^2\psi+V(x,y)\psi+\gamma|\psi|^2\psi, \quad (1)$$

where ∇_{\perp}^2 is the Laplace operator in the (x, y) plane, $V(x, y)$ is the double-well potential measured in units of $\hbar\omega_z$, and $\gamma=8\pi a/r_z$ is the effective atomic interaction coefficient given by the s -wave scattering length a .

II. LINEAR DOUBLE-WELL TUNNELING THEORY

We initially consider a linear regime ($\gamma=0$) which is possible to obtain by properly adjusting the Feshbach resonances, and take a two-dimensional potential consistent in a double well with a shape given by two displaced Gaussian functions,

$$V(x, y)=-V_l \exp\left[-\frac{(x-d/2)^2+y^2}{w_l^2}\right]-V_r \exp\left[-\frac{(x+d/2)^2+y^2}{w_r^2}\right], \quad (2)$$

where V_l and V_r are the depth and w_l and w_r the width of each well of the potential and d the separation between them. This configuration can be easily achieved with an optical dipole trap generated with a CO₂ laser beam [17,18]. Such a potential supports stationary states or modes of the form

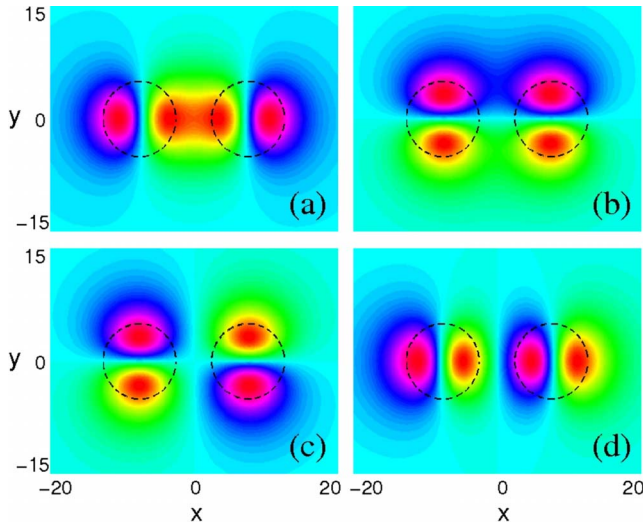


FIG. 1. (Color online) The four stationary states or modes supported by a double well with Gaussian profile, presenting a nodal line on each of the wells. Subfigures (a)–(d) correspond to stationary states $|f_1\rangle$ – $|f_4\rangle$. Dashed lines indicate the well border measured at the points where the amplitude is $1/e$ of the minimum. Zones in red-blue tones (dark gray) are positive lobes while those in red-yellow-green tones (bright gray) correspond to negative lobes.

$\psi(x, y, \tau) = f(x, y) \exp(-i\mu\tau)$, where μ is the energy of the state and $f(x, y)$ is a real-valued function only dependent on the spatial variables, which satisfies

$$\mu f = -\nabla_{\perp}^2 f + V(x, y)f. \quad (3)$$

We are interested in the modes having one nodal line located at the position of each of the wells, since in that case an appropriate linear combination of those states originates vortex-type states of the lowest vorticity, $\ell=1$, on each of the separate wells. As it is known, due to symmetry reasons, there are only four modes with a unique nodal line on each well position, forming a set that we denote as $\mathcal{D} = \{|f_1\rangle, |f_2\rangle, |f_3\rangle, |f_4\rangle\}$ and plot in Fig. 1. These modes are nondegenerated due to the breaking of the $O(2)$ symmetry into a C_{2v} symmetry produced by the double well. In spite of this symmetry lift, it is still possible to build vortex-type states choosing suitable linear combinations. In fact, there

are four vortex-type states given by the following combinations of the basis states of set \mathcal{D} :

$$|l+\rangle = (1/2)(|f_1\rangle + i|f_2\rangle + i|f_3\rangle + |f_4\rangle), \quad (4)$$

$$|l-\rangle = (1/2)(|f_1\rangle - i|f_2\rangle - i|f_3\rangle + |f_4\rangle), \quad (5)$$

$$|r+\rangle = (1/2)(-|f_1\rangle + i|f_2\rangle - i|f_3\rangle + |f_4\rangle), \quad (6)$$

$$|r-\rangle = (1/2)(-|f_1\rangle - i|f_2\rangle + i|f_3\rangle + |f_4\rangle). \quad (7)$$

In the above expressions we have denoted as l and r the states with a vortex in the left and right well, respectively, and as $+$ ($-$) those with positive (negative) vorticity. In order to illustrate the construction of these vortex states we have plotted in Fig. 2 the modulus and phase of such linear combinations, showing each one a single vortex located in one of the wells, as well as a negligible remanent on the other well.

Since the states forming the basis set are nondegenerated, those linear combinations are not stationary states and change with time in a complex way. The spectrum of states with angular momentum $\ell=1$ for two infinitely separated potential wells is formed by the degenerated quadruplet $|l\pm\rangle, |r\pm\rangle$. As the distance between the wells decreases, the degeneracy becomes broken and first-order degenerated perturbation theory applies, resulting that the time evolution of the field can be described at any instant τ as a linear combination of the states of the basis set \mathcal{D} , $|\psi(\tau)\rangle = c_1(\tau)|f_1\rangle + c_2(\tau)|f_2\rangle + c_3(\tau)|f_3\rangle + c_4(\tau)|f_4\rangle$, where the time-dependent coefficients are $c_j(\tau) = c_j(0) \exp(i\mu_j\tau)$, μ_j being the energy of the state $|f_j\rangle$.

The system evolution will reach a double vortex or whatever desired final state $|u\rangle$ at some particular instants, for which the condition $|\langle u|\psi\rangle|=1$ is fulfilled, assuming that both fields are normalized. As an example, we will focus on the case of obtaining a double vortex with opposite vorticity, i.e., the final state $|u\rangle = \exp(i\theta)(|l+\rangle - i|r-\rangle)/\sqrt{2}$, where $\exp(i\theta)$ is a global arbitrary phase factor. Besides, if we start with a single vortex in the left core $|\psi(0)\rangle = |l+\rangle$, the projection on the final desired state will produce,

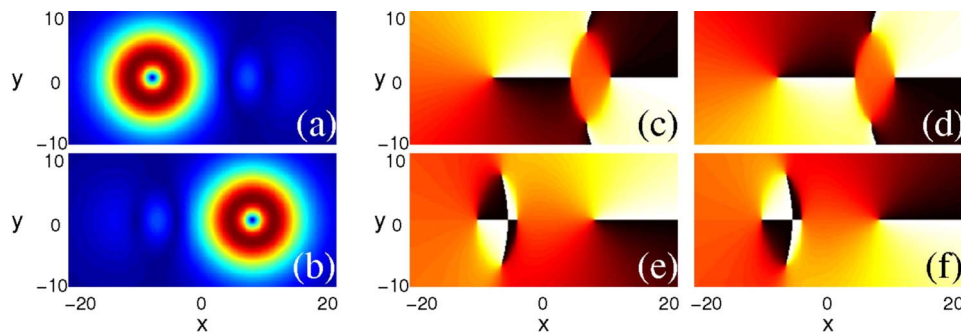


FIG. 2. (Color online) Vortex-type states constructed as linear combinations of the four modes of the double-well potential presenting a nodal line. (a-b) shows the amplitude for the combinations resulting in a vortex on the left well ($|l+\rangle$ and $|l-\rangle$) and the right well ($|r+\rangle$ and $|r-\rangle$), respectively. Subfigures (c)–(f) show the phase distribution for the different states $|l+\rangle$, $|l-\rangle$, $|r+\rangle$, and $|r-\rangle$, respectively.

$$\begin{aligned} |\langle u | \psi(\tau) \rangle| &= (1/4) |\exp(i\mu_1\tau) + \exp(i\mu_2\tau) + i \exp(i\mu_3\tau) \\ &\quad + i \exp(i\mu_4\tau)|, \end{aligned} \quad (8)$$

and will be identically the unity when the following conditions are simultaneously satisfied:

$$\mu_1\tau = \mu_2\tau + q(2\pi), \quad (9)$$

$$\mu_1\tau = \mu_3\tau + (4r+1)(\pi/2), \quad (10)$$

$$\mu_1\tau = \mu_4\tau + (4s+1)(\pi/2), \quad (11)$$

being $q, r, s \in \mathbb{Z}$. These equations can be written as

$$\frac{4q}{4r+1} = \frac{\mu_1 - \mu_2}{\mu_1 - \mu_3} = \xi, \quad (12)$$

$$\frac{4q}{4s+1} = \frac{\mu_1 - \mu_2}{\mu_1 - \mu_4} = \zeta, \quad (13)$$

so that, in order that the conditions can be fulfilled, it is required that the quotients above are rational numbers. This is always met when the energies are obtained numerically, but even in the case they were irrational it is always possible to find a rational number as closest as desired. This analysis demonstrates that an instant where the final state is obtained always exists provided that the potential parameters make the wells to support the first excited azimuthal state (vortex), although it may happen for a very long evolution time. Nevertheless, a perfect match of the desired state is not requested in practice, just being enough reaching a projection value little lower than unity.

III. NUMERICAL SIMULATIONS

In order to confirm the theory developed in the previous section, we have performed a set of simulations, propagating a vortex initially located at one of the potential minima, $|\psi_0\rangle$, by means of a finite-difference Crank-Nicolson algorithm. In principle we can chose one of the linear combinations given by Eqs. (4)–(7) as a starting field. Nevertheless, in order to be more realistic, we chose a stationary state of a single-well (Gaussian) potential located on one of the well positions. This state is not a stationary state of the double-well potential and consequently a slightly matter leak is produced at the beginning of the propagation. Due to the weak coupling between both wells, the matter expelled is, however, negligible and the use of transparent boundary conditions allow to get rid of it through the domain edges avoiding further interference. A simple Gaussian vortex profile of the same width as the potential well would also work fine instead of the single-well stationary state.

We will focus on the particular case of obtaining a replication of the initial vortex with opposite vorticity, though every other final state could be searched for. In that way, the normalized fields centered at each potential minima for the final state should be $|u_l\rangle = |\psi_0\rangle = |\alpha_1\rangle + i|\alpha_2\rangle$ and $|u_r\rangle = |\alpha_1\rangle - i|\alpha_2\rangle$, where $|\alpha_1\rangle$ and $|\alpha_2\rangle$ are the two degenerated dipole states of the single well. For these and all further simulations

we took the values $V_l = V_r = 0.5$, $w_l = w_r = 5$, and $d = 15$ for the potential parameters, which assure that the wells support the first-order azimuthal excited state (vortex). The evolution was tracked by evaluating at each step how similar is the present state to the one we would eventually like to achieve. In order to quantify this similarity we consider the probability of finding the desired vortex at each potential minima, projecting the propagating field over the desired states $P_{l,r} = |\langle u_{l,r} | \psi \rangle|^2$. The probability of simultaneously forming a vortex in both potential wells is consequently described by the joint probability,

$$\eta = P(u_l \cap u_r) = P(u_l)P(u_r) = |\langle u_l | \psi \rangle|^2 |\langle u_r | \psi \rangle|^2. \quad (14)$$

We regard η as the *replication parameter*, valued between 0 and 1.

In Figs. 3(a) and 3(b) parameter η is plotted as a function of the normalized evolution time, τ , for two different values of the well separation d . The shape is a succession of peaks each one reaching a different value. A reasonable rate of replication is achieved for $\eta > 0.9$ as shown in the snapshots of Fig. 3(c), corresponding to the highest peaks which overpass such value, the result having a particular good appearance for the peak labeled B, which reaches almost the unity. Comparing both graphs for the two different values of d , it can be appreciated that basically they present the same peaks, but located at different positions on the τ axis (shifted to earlier times) and reaching different values. This fact encourages to make a study of the behavior of parameter η as a function of the separation of the two potential minima to determine if the replication may take place for shorter evolution times.

In Fig. 4 the τ position for three of the peaks in Fig. 3 and the peak value of parameter η is plotted as a function of the well separation. Figure 4(a) confirms the shift of the peaks to lower evolution times when the two potential maxima get closer, and Fig. 4(b) shows that for each of the peaks there is a value of d which gives rise to a maximum value of η at some instant. In that way, acting on the well separation d allows us to modify and determine the instant at which we obtain the desired result. Even so, the necessary evolution time is generally too long compared with the typical mean life of the condensate, and also the instant for which the replication is obtained is so critical that the replicated state is quickly lost in the subsequent well separation process.

It is worth a brief remark about the flux conservation in this system, which is directly related to the winding number defined as the contour integral along a closed curve containing the condensates. Its conservation in discrete-symmetry media, like the double-well potential, is still an open question. The winding number can be related to a quantity called angular-pseudomomentum [19,20] which is connected with the symmetry order of the system. For states with well-defined angular-pseudomomentum, we showed numerically that both the winding number and the angular-pseudomomentum are conserved [19,21,22]. However, the initial state composed by a single-charged vortex has a well-defined winding number but not a well-defined angular-pseudomomentum. Consequently, the conservation of the winding number, or equivalently the total flux, cannot be

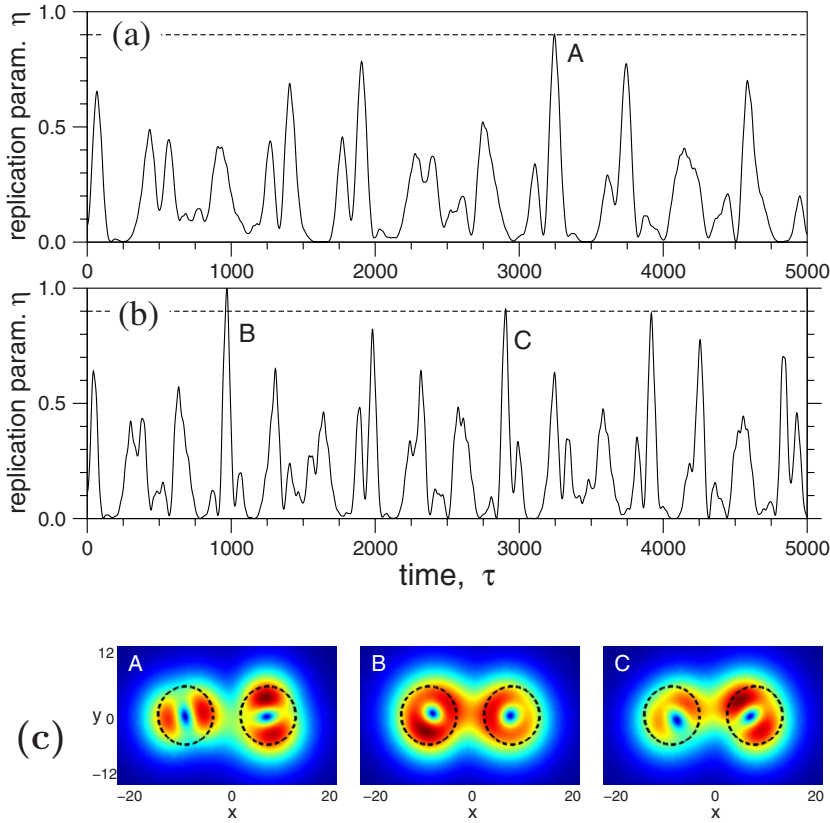


FIG. 3. (Color online) Time evolution of the replication parameter η , starting from a single vortex state located on one of the potential minima for two well separation distances: $d=15$ (a) and $d=13.7$ (b). (c) Some snapshots illustrating the system state for two different times: labels correspond to those of the peaks in (a) and (b).

assured. Further numerical and theoretical analysis is yet to be done to address this question.

IV. FAST REPLICATION, SEPARATION, AND RECOVERING

In order to separate both vortices generated at each potential minima a potential barrier is initially placed between them to stop matter tunneling. Then, a process of adiabatic separation of the potential wells is carried out, slightly

changing the potential at each propagation step, so that both wells maintain the shape but increase the separation slowly. This slow (or adiabatic) separation is necessary to assure that the vortices are trapped in the well minima at all times. The separation of the vortices is performed up to a position where they are far away enough to stop matter transfer and only then the potential barrier is removed. This strategy avoids matter transfer during the process but introduces perturbations in the potential which make the phase between the two dipole states of each vortex to evolve, destroying the desired vortex structure. Nevertheless, since the perturbations affect

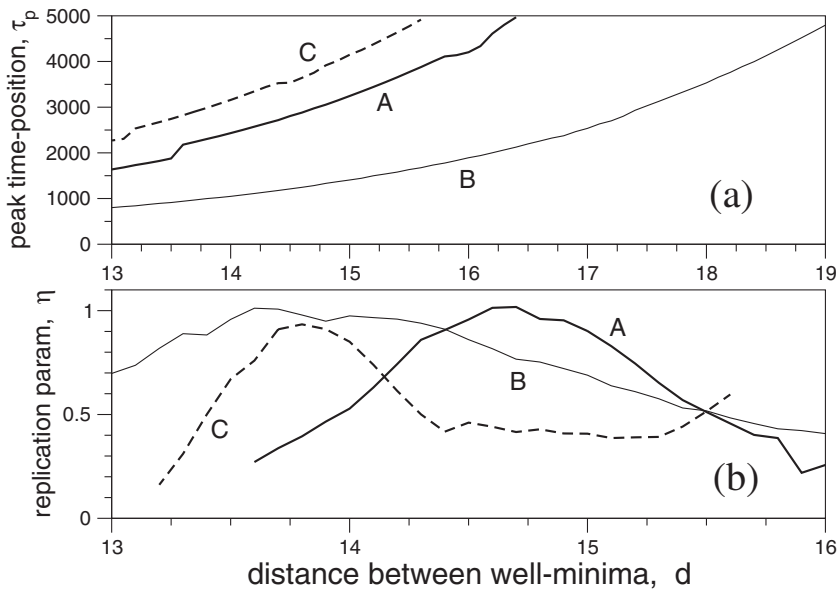


FIG. 4. (a) Dependence of the peak position in time (a) and magnitude (replication parameter η) of the peak (b) versus separation between the potential minima. Labels A, B, and C correspond to the peaks of the same label in Fig. 3.

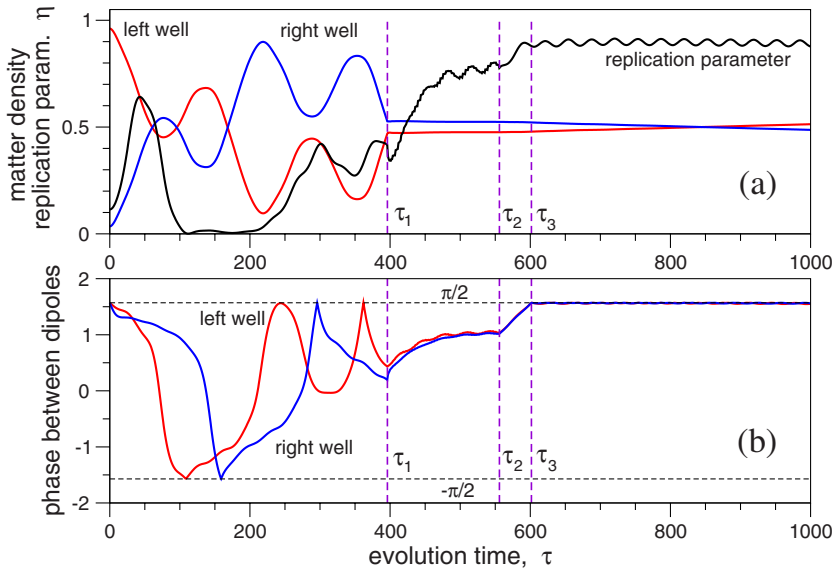


FIG. 5. (Color online) (a) Matter density for each potential minimum and replication parameter as functions of the normalized time for a simulation in a nonlinear regime. (b) Evolution of the phase difference between real and imaginary parts of the field (dipoles) for each potential minimum.

only to the relative phase and not to the atom-density distribution between the dipoles, vortices are easy to recover by inducing a small distortion in each of the potential wells, say, making them slightly elliptic instead of cylindrically symmetric. This asymmetry makes the dipoles nondegenerated states of the single well and an evolution with different characteristic energies is produced. Consequently, the relative phase also evolves and it can be monitored up to the point where it reaches the value $\pi/2$. At this point the cylindrically symmetric shape of the wells is restored and consequently the relative phase evolution stops and the final replicated vortices are obtained.

This possibility of recovering the vortex states is the key to achieve the desired replication in a much faster way. In fact, achieving exactly replicated vortices is unnecessary before starting the well-separation process, since the vortex states can be subsequently regenerated from other field structures by means of the deformation of the single-well potentials. There are only two necessary conditions to meet at the end of the evolution process. First, the matter should be equally distributed between each potential minimum and second, the matter at each minimum should be equally distributed between both dipole states. Besides, the latter condition

can be always fulfilled provided each elliptic well is established with the suitable axes orientation to match the nodal lines of the dipole basis set. We remark that all these complementary techniques to split and recover the vortices are easy to implement experimentally.

To demonstrate the effectiveness of these combined techniques for vortex replication, in Figs. 5 and 6 we show the results of a simulation performed for a most general case of a nonlinear regime ($\gamma=1$). In Fig. 5(a), the matter density at both potential minima as well as the replication parameter η are plotted. Figure 6 shows real time values for the case of a $r_z=1 \mu\text{m}$ thick condensate made of Rb atoms. The matter tunneling process is stopped at instant τ_1 [Fig. 6(c)], when the matter density is approximately equidistributed between both wells. At this instant, a potential barrier (amplitude 20, width 0.5) is established between the wells to stop matter transfer as can be seen in Fig. 5(a) and the wells start to be adiabatically separated. The well separation completes at instant τ_2 [Fig. 6(d)]. At this instant, the barrier is suppressed, and each well is distorted into an elliptic shape (eccentricity 0.4) between instants τ_2 and τ_3 to recover the $\pi/2$ phase between dipole states and consequently the vortex structure at τ_3 [Fig. 6(e)]. This is possible for this particular case if the

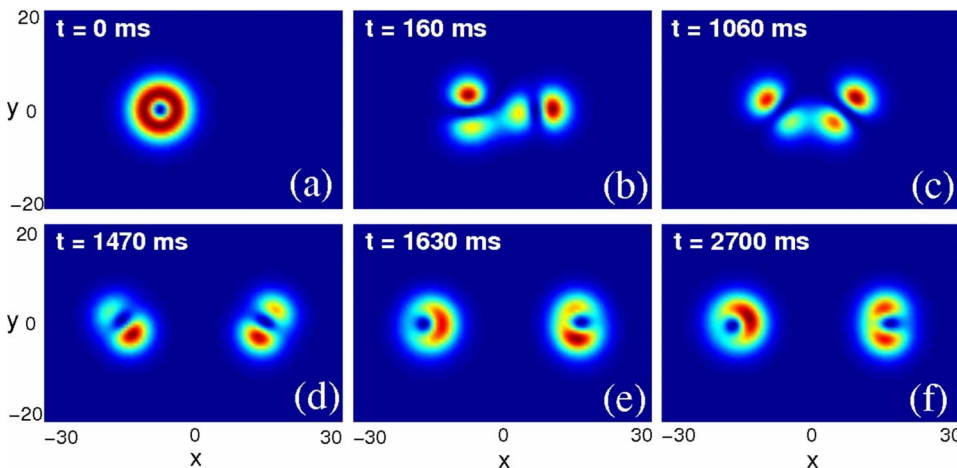


FIG. 6. (Color online) Sequence of different photograms showing a vortex replication in nonlinear regime. (c), (d), and (e) correspond to times τ_1 , τ_2 , and τ_3 , respectively in Fig. 5. Overprinted is the real time $t=\tau/\omega_z$ corresponding to every snapshot for the case of a $r_z=1 \mu\text{m}$ thick condensate of Rb atoms.

ellipse axes coincide with the Cartesian ones, since the matter density is equally distributed between both associated dipoles, as is seen in Fig. 6(d). The phase evolution for each vortex is shown in Fig. 5(b) where the relative phase between dipoles is plotted for both potential wells. At instant τ_3 the cylindrical symmetry of the potential wells is restored and the vortices remain stable from that point on. The plots show the evolution up to fairly later times to account for this [Fig. 6(f)]. It is important to notice that the 50% matter transfer to the second well is even achieved at earlier times than τ_1 as shown in Fig. 5(a) (points at which both density lines cross) and the vortices could be restored from those points—as for example from the instant shown in Fig. 6(b)—if the ellipticity induced in each well potential is tuned to have the adequate axes orientation for both single-well dipoles to equally share the matter density.

V. CONCLUSIONS

We have determined the analytically conditions in the linear regime for splitting a Bose-Einstein condensate vortex,

initially located in one minimum of a double well, into two equal vortex copies each located in different minima or whatever final state that was desired. The replication technique has been demonstrated in a nonlinear general case with numerical simulations and complemented with a vortex-recovering strategy, consisting in an easy and experimentally feasible modification of the potential shape that allows to dramatically decrease the replication time.

ACKNOWLEDGMENTS

This work was supported by Ministerio de Educación y Ciencia of Spain (Projects No. FIS2007-62560, No. BFM2003-02832, No. TIN2006-12890, No. FIS2005-01189, and network No. FIS2007-29090-E and Ramón y Cajal contract granted to J.R.S.), Xunta de Galicia, Spain (Project No. PGIDIT06PXIB239155PR), and Generalitat Valenciana, Spain (Project No. GV2008-032 and Contract No. APOSTD/2007/052 granted to M.Z.).

-
- [1] K. W. Madison, F. Chevy, W. Wohlleben, and J. Dalibard, *Phys. Rev. Lett.* **84**, 806 (2000).
 - [2] M. R. Matthews, B. P. Anderson, P. C. Haljan, D. S. Hall, C. E. Wieman, and E. A. Cornell, *Phys. Rev. Lett.* **83**, 2498 (1999).
 - [3] A. E. Leanhardt, A. Görlitz, A. P. Chikkatur, D. Kielpinski, Y. Shin, D. E. Pritchard, and W. Ketterle, *Phys. Rev. Lett.* **89**, 190403 (2002).
 - [4] J. R. Abo-Shaeer, C. Raman, J. M. Vogels, and W. Ketterle, *Science* **292**, 476 (2001).
 - [5] V. Schweikhard, I. Coddington, P. Engels, S. Tung, and E. A. Cornell, *Phys. Rev. Lett.* **93**, 210403 (2004).
 - [6] I. Coddington, P. C. Haljan, P. Engels, V. Schweikhard, S. Tung, and E. A. Cornell, *Phys. Rev. A* **70**, 063607 (2004).
 - [7] B. P. Anderson, P. C. Haljan, C. E. Wieman, and E. A. Cornell, *Phys. Rev. Lett.* **85**, 2857 (2000).
 - [8] B. Y. Rubinstein and L. M. Pismen, *Physica D* **78**, 1 (1994).
 - [9] P. Mason and N. G. Berloff, *Phys. Rev. A* **77**, 032107 (2008).
 - [10] M. Albiez, R. Gati, J. Fölling, S. Hunsmann, M. Cristiani, and M. K. Oberthaler, *Phys. Rev. Lett.* **95**, 010402 (2005).
 - [11] S. Fölling, S. Trotzky, P. Cheinet, M. Feld, R. Saers, A. Widera, T. Müller, and I. Bloch, *Nature (London)* **448**, 1029 (2007).
 - [12] P. Ghosh and F. Sols, *Phys. Rev. A* **77**, 033609 (2008).
 - [13] T. Schumm, S. Hofferberth, L. M. Anderson, S. Wildermuth, S. Groth, I. Bar-Joseph, J. Schmiedmayer, and P. Krüger, *Nat. Phys.* **1**, 57 (2005).
 - [14] M. Zhang, P. Zhang, M. S. Chapman, and L. You, *Phys. Rev. Lett.* **97**, 070403 (2006).
 - [15] C. Lee, E. A. Ostrovskaya, and Y. Kivshar, *J. Phys. B* **40**, 4235 (2007).
 - [16] V. M. Pérez-García, H. Michinel, and H. Herrero, *Phys. Rev. A* **57**, 3837 (1998).
 - [17] D. M. Stamper-Kurn, M. R. Andrews, A. P. Chikkatur, S. Inouye, H.-J. Miesner, J. Stenger, and W. Ketterle, *Phys. Rev. Lett.* **80**, 2027 (1998).
 - [18] J. P. Martikainen, *Phys. Rev. A* **63**, 043602 (2001).
 - [19] A. Ferrando, *Phys. Rev. E* **72**, 036612 (2005).
 - [20] M. A. García-March, A. Ferrando, M. Zacarés, J. Vijande, and L. D. Carr, e-print arXiv:0806.0947.
 - [21] A. Ferrando, M. Zacarés, M. A. García-March, J. A. Monsoriu, and P. F. de Córdoba, *Phys. Rev. Lett.* **95**, 123901 (2005).
 - [22] M. Zacarés, M. A. García-March, J. Vijande, A. Ferrando, and E. Merino, e-print arXiv:0811.0667.